Advanced Oxide Material Systems for 1650 °C Thermal/Environmental Barrier Coating Applications

Dongming Zhu
U.S. Army Research Laboratory, Glenn Research Center, Cleveland, Ohio

Dennis S. Fox, Narottam P. Bansal, and Robert A. Miller
Glenn Research Center, Cleveland, Ohio

Since its founding, NASA has been dedicated to the advancement of aeronautics and space science. The NASA Scientific and Technical Information (STI) Program Office plays a key part in helping NASA maintain this important role.

The NASA STI Program Office is operated by Langley Research Center, the Lead Center for NASA's scientific and technical information. The NASA STI Program Office provides access to the NASA STI Database, the largest collection of aeronautical and space science STI in the world. The Program Office is also NASA's institutional mechanism for disseminating the results of its research and development activities. These results are published by NASA in the NASA STI Report Series, which includes the following report types:

- TECHNICAL PUBLICATION. Reports of completed research or a major significant phase of research that present the results of NASA programs and include extensive data or theoretical analysis. Includes compilations of significant scientific and technical data and information deemed to be of continuing reference value. NASA's counterpart of peer-reviewed formal professional papers but has less stringent limitations on manuscript length and extent of graphic presentations.

- TECHNICAL MEMORANDUM. Scientific and technical findings that are preliminary or of specialized interest, e.g., quick release reports, working papers, and bibliographies that contain minimal annotation. Does not contain extensive analysis.

- CONTRACTOR REPORT. Scientific and technical findings by NASA-sponsored contractors and grantees.

- CONFERENCE PUBLICATION. Collected papers from scientific and technical conferences, symposia, seminars, or other meetings sponsored or cosponsored by NASA.

- SPECIAL PUBLICATION. Scientific, technical, or historical information from NASA programs, projects, and missions, often concerned with subjects having substantial public interest.

- TECHNICAL TRANSLATION. English-language translations of foreign scientific and technical material pertinent to NASA's mission.

Specialized services that complement the STI Program Office's diverse offerings include creating custom thesauri, building customized databases, organizing and publishing research results . . . even providing videos.

For more information about the NASA STI Program Office, see the following:

- Access the NASA STI Program Home Page at *http://www.sti.nasa.gov*

- E-mail your question via the Internet to help@sti.nasa.gov

- Fax your question to the NASA Access Help Desk at 301–621–0134

- Telephone the NASA Access Help Desk at 301–621–0390

- Write to:
  NASA Access Help Desk
  NASA Center for AeroSpace Information
  7121 Standard Drive
  Hanover, MD 21076

NASA/TM—2004-213219

ARL–TR–3298

Advanced Oxide Material Systems for 1650 °C Thermal/Environmental Barrier Coating Applications

Dongming Zhu
U.S. Army Research Laboratory, Glenn Research Center, Cleveland, Ohio

Dennis S. Fox, Narottam P. Bansal, and Robert A. Miller
Glenn Research Center, Cleveland, Ohio

National Aeronautics and
Space Administration

Glenn Research Center

December 2004

Acknowledgments

Advanced Oxide Material Systems for 1650 °C Thermal and Environmental Barrier Coating Applications

Dongming Zhu
U.S. Army Research Laboratory
National Aeronautics and Space Administration
Glenn Research Center
Cleveland, Ohio 44135

Dennis S. Fox, Narottam P. Bansal, and Robert A. Miller
National Aeronautics and Space Administration
Glenn Research Center
Cleveland, Ohio 44135

Summary

Advanced thermal and environmental barrier coatings (TEBCs) are being developed for low-emission SiC/SiC ceramic matrix composite (CMC) combustor and vane applications to extend the CMC liner and vane temperature capability to 1650 °C (3000 °F) in oxidizing and water-vapor-containing combustion environments. The advanced 1650 °C TEBC system is required to have a better high-temperature stability, lower thermal conductivity, and more resistance to sintering and thermal stress than current coating systems under engine high-heat-flux and severe thermal cycling conditions. In this report, the thermal conductivity and water vapor stability of selected candidate hafnia-, pyrochlore-, and magnetoplumbite-based TEBC materials are evaluated. The effects of dopants on the materials' properties are also discussed. The test results have been used to downselect the TEBC materials and help demonstrate the feasibility of advanced 1650 °C coatings with long-term thermal cycling durability.

Introduction

Thermal and environmental barrier coatings (TEBCs) will play a crucial role in advanced gas turbine engine systems because of their ability to significantly increase engine operating temperature and reduce cooling requirements, thus greatly help to achieve engine low emission and high efficiency goals. Under the NASA Ultra-Efficient Engine Technology (UEET) Program, advanced TEBC systems are being developed to provide vital thermal and environmental protection for Si-based ceramic components at gas temperatures exceeding 1760 °C (3200 °F) in harsh combustion environments. The TEBC system is required to have good phase stability, low lattice and radiation thermal conductivity, and high resistance to sintering and thermal stress under the engine high-heat-flux and severe thermal cycling conditions. Advanced heat-flux testing approaches (refs. 1 to 8) have also been established for the 1650 °C coating development. A simulated combustion environment with water vapor has also been incorporated into the heat-flux test capabilities (ref. 3).

In this report, thermal conductivity and water vapor stability of selected HfO_2, pyrochlore, and magnetoplumbite oxide-based materials are evaluated at temperatures up to 1650 °C using a steady-state laser heat-flux technique, and water vapor thermogravimetric analysis (TGA), respectively. Sintering behavior and thermal cycling durability of the plasma-sprayed coatings were determined by monitoring the thermal conductivity changes during the laser heat-flux testing.

Materials and Experimental Methods

Materials

The test specimens of hafnia (HfO_2), pyrochlore ($A_2B_2O_7$), and magnetoplumbite ($AMgAl_{11}O_{19}$) oxide materials (where A and B refer to rare earths and zirconium or hafnium, respectively, see table I) were either hot-pressed disks (25.4 mm in diameter, 2 to 4 mm in thickness) or plasma-sprayed coatings (254 to 400 µm in thickness). Spray-dried oxide powders were hot pressed at 1500 °C for an hour under 30 MPa pressure primarily in a graphite die. Sol-gel-derived pyrochlore and magnetoplumbite powders were also used to make hot-pressed specimens.

TABLE I.—OXIDE MATERIALS INVESTIGATED FOR
ADVANCED THERMAL AND ENVIRONMENTAL
BARRIER COATING SYSTEMS

Hafnia-based ceramics (HfO_2-A_2O_3)	
HfO_2-5 mol% Y_2O_3	(5YSHf)
HfO_2-10 mol% Y_2O_3	(10YSHf)
HfO_2-15 mol% Y_2O_3	(15YSHf)
HfO_2-20 mol% Y_2O_3	(20YSHf)
HfO_2-25 mol% Y_2O_3	(25YSHf)
HfO_2-18 mol% $(Y,Gd,Yb)_2O_3$	(Multicomponent)
Pyrochlores ($A_2B_2O_7$)	**Magnetoplumbites ($AMgAl_{11}O_{19}$)**
$La_2Hf_2O_7$	$LaMgAl_{11}O_{19}$
$La_2Zr_2O_7$	$SmMgAl_{11}O_{19}$
$(La,Gd)_2Zr_2O_7$	$GdMgAl_{11}O_{19}$
$(La,Yb)_2Zr_2O_7$	$(Gd,Yb)MgAl_{11}O_{19}$
$(La,Gd,Yb)_2Zr_2O_7$	

The coating specimens were prepared by plasma spraying the spray-dried, and plasma-reacted powders on either metallic, SiC Hexoloy (Saint-Gobain Ceramics, Niagara Fall, NY), and/or melt infiltrated (MI) SiC/SiC ceramic matrix composite (CMC) substrates (GE Power Systems, NY). For thermal conductivity measurements, the ceramic coating specimens with the low-pressure-plasma-sprayed NiCrAlY bond-coated René N5 (General Electric Company, Fairfield, CT) nickel-base superalloy substrates (25.4 mm in diameter and 3.2 mm in thickness) were used. On the other hand, for 1650 °C sintering and thermal cycling durability testing, complete TEBC coating systems—consisting of layers of the top oxide coating and then either mullite or a mullite-barium strontium aluminosilicate (BSAS) mixture on a silicon coating—were prepared with either the MI SiC/SiC CMC (25.4 mm in diameter, 2.2 mm in thickness) or Hexoloy SiC (25.4 mm in diameter, 3.17 mm in thickness) substrates. The phase structures of the coating materials were examined using x-ray diffraction.

Thermal Conductivity and Thermal Gradient Cyclic Testing

Thermal conductivity testing of hafnia, pyrochlore, and magnetoplumbite hot-pressed and coating specimens was carried out using a 3.5 kW CO_2 laser (wavelength 10.6 µm) high-heat-flux rig. The general test approaches have been described elsewhere (refs. 1 to 4). In this steady-state laser heat-flux thermal conductivity test, the specimen surface heating was provided by the laser beam, and backside air cooling was used to maintain desired specimen temperatures. A uniform laser heat flux was obtained over the 23.9-mm-diameter aperture region of the specimen surface using a beam integrating ZnSe lens with either specimen or lens rotation. Platinum wire flat coils (wire diameter 0.38 mm) were used to form

thin air gaps between the top aluminum aperture plate and stainless steel back plate to minimize the specimen heat losses through the fixture. The thermal conductivities of the hot-pressed and coating specimens were determined from the pass-through heat flux and measured temperature difference through the ceramic specimen (or the ceramic coating) thickness under the steady-state laser heating or thermal cycling conditions by a one-dimensional heat transfer model.

Thermal gradient cyclic testing was conducted for selected HfO_2-based coating systems to evaluate coating durability. As in the laser thermal conductivity test, the uniformly distributed laser heat flux was delivered to the coating specimen surface to provide the specimen heating. The required specimen temperatures and thermal gradients were achieved by controlling the delivered laser heat flux and backside air cooling. In the present study, the surface temperature was controlled at 1650 °C and the interface temperature at approximately 1316 °C, and 30-min heating and 3-min cooling cycles were used for the thermal cycling. Thermal conductivity of the coating systems was measured in situ as a function of cycle time to monitor the coating cyclic response.

Water Vapor Stability Testing

The water-vapor stability of these oxide materials was investigated using thermogravimetric analysis (TGA) at 1650 °C, in a 50-50 percent flowing H_2O-O_2 environment. Samples were suspended on sapphire hangers inside a 2.5-cm one-dimensional vertical alumina furnace tube (998A, Vesuvius McDanel, Beaver Falls, PA). Water-vapor-laden oxygen was introduced into the furnace tube using an apparatus described elsewhere (ref. 9). Weight change was continuously monitored with a recording microbalance (C–1000, Cahn Instruments, Cerritos, CA), and specific weight gain and loss (mg/cm^2) were measured as a function of time. The linear specific weight change rate constants were obtained from the specific weight change curves of the materials after 100 h of testing.

Results and Discussion

Thermal Conductivity of Hot-Pressed Specimens

Figure 1 shows the thermal conductivity measurement results of the HfO_2-Y_2O_3 hot-pressed specimens. As shown in figure 1(a), the HfO_2 materials generally showed a conductivity decrease with an increase in temperature. A previous study showed that thermal conductivity typically showed less temperature dependence with a higher Y_2O_3 dopant content (ref. 8). The conductivity increases with temperature in the high-temperature regime can be attributed to the increased radiation heat flux, which will result in the increased apparent thermal conductivity. Figure 1(b) shows measured density and thermal conductivity at 1400 °C of the HfO_2 hot-pressed specimens as a function of Y_2O_3 concentration. The density of the HfO_2 specimens was relatively low (i.e., the porosity was relatively high) due to the relatively large particle size powder used. The conductivity data scatter observed was due to the variation in porosity in these hot-processed specimens, with the lower density specimens having lower measured conductivity. Nevertheless, the specimen thermal conductivity showed a general trend to decrease with increase in the yttria dopant concentration. The multicomponent HfO_2-18 mol% $(Y,Gd,Yb)_2O_3$ coatings specimen showed lower thermal conductivity as compared to the HfO_2-Y_2O_3 coatings at a given total dopant concentration.

Figure 2(a) shows thermal conductivity of $La_2Zr_2O_7$ (pyrochlore $A_2B_2O_7$ structure) hot-pressed specimens as a function of surface test temperature. The $La_2Zr_2O_7$ specimens had low porosity due to the small particle sizes of $La_2Zr_2O_7$ powder used to process them. In particular, the specimens fabricated with the sol-gel derived powder achieved the theoretical density. These high-density, low-porosity $La_2Zr_2O_7$
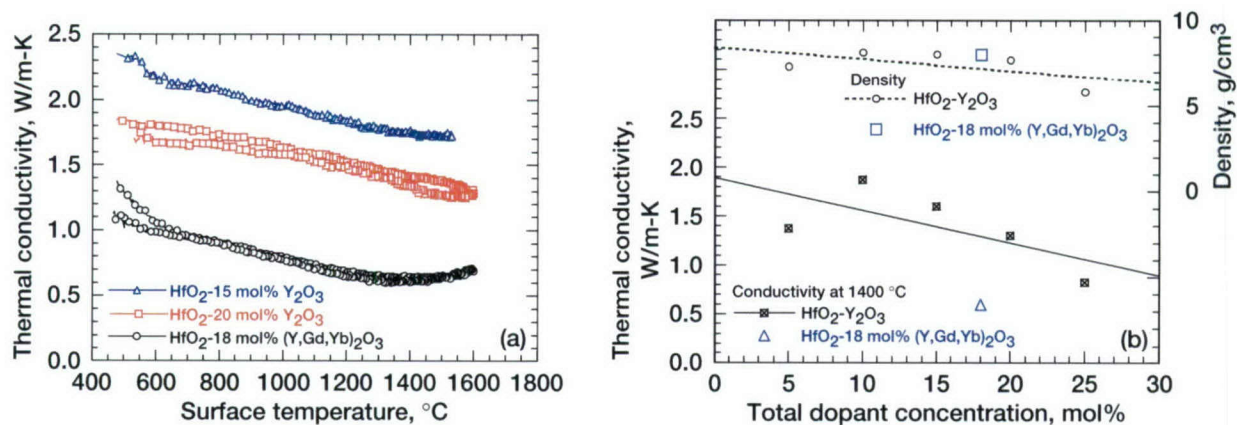
Figure 1.—Measured thermal conductivity of hot-pressed HfO_2-based oxides. (a) HfO_2-Y_2O_3 as function of temperature. (b) HfO_2 as function of dopant concentration.
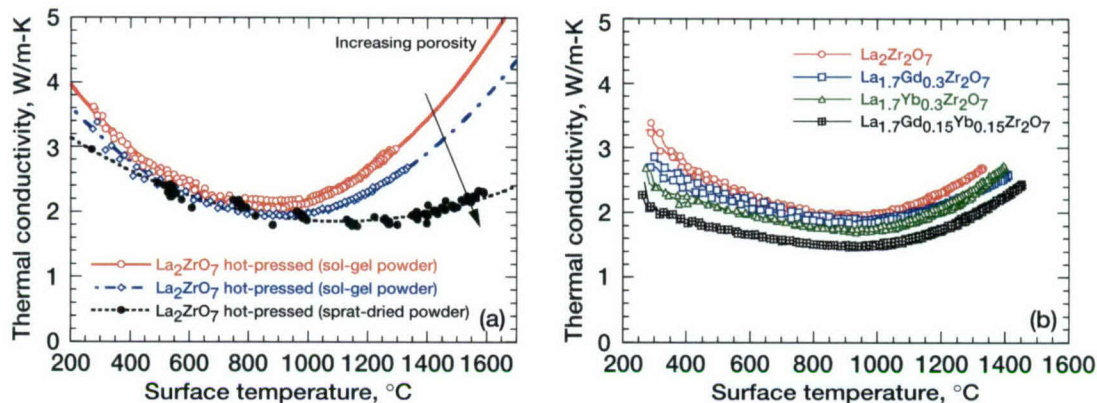

Figure 2.—Thermal conductivity of dense $La_2Zr_2O_7$-based hot-pressed specimens as function of surface test temperature. (a) Specimens of differing porosity. (b) Specimens with differing dopants of similar porosity.

specimens showed significant thermal conductivity increases starting at 900 °C because of the increased radiation contribution with increasing temperature. The small amount of microporosity in the spray-dried powder-processed specimen did not affect the lattice thermal conductivity dramatically. However, the microporosity in the specimen significantly reduced the radiation conductivity as compared to the almost pore-free, sol-gel powder-processed specimens. The conductivity increased by more than 100 percent for the very dense specimens because of the increased radiation heat transfer under thermal gradient conditions. Figure 2(b) shows that the rare earth-oxide-doped pyrochlores $La_{1.7}Gd_{0.3}Zr_2O_7$, $La_{1.7}Yb_{0.3}Zr_2O_7$, and $La_{1.7}Gd_{0.15}Yb_{0.15}Zr_2O_7$ had lower thermal conductivity than the undoped $La_2Zr_2O_7$. The Gd_2O_3 and Yb_2O_3 co-doped materials showed the lowest thermal conductivity.

Figure 3 shows thermal conductivity of hot-pressed magnetoplumbite-type oxide specimens as a function of surface test temperature. The material conductivity exhibited little temperature dependence. It also seemed that $GdMgAl_{11}O_{19}$ and $SmMgAl_{11}O_{19}$ had lower thermal conductivity than $LaMgAl_{11}O_{19}$, as shown in figure 3(a). In addition, similar to the HfO_2 and pyrochlore oxides, the rare earth-doped $Gd_{0.7}Yb_{0.3}MgAl_{11}O_{19}$ had the lowest thermal conductivity, as shown in figure 3(b).
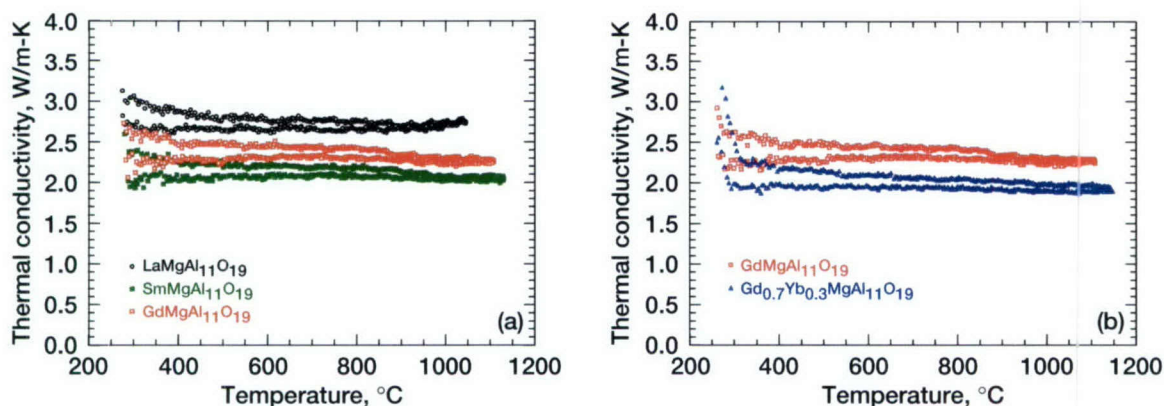
Figure 3.—Thermal conductivity of hot-pressed magnetoplumbite specimens as function of surface test temperature. (a) Showing effect of rare earth component. (b) Showing effect of co-doping.

Thermal Conductivity of Plasma-Sprayed Coatings

Figure 4 shows the thermal conductivity change kinetics of plasma-sprayed HfO_2-Y_2O_3 coatings, coated on SiC hexoloy substrate, tested at 1650 °C with the pass-through heat flux in the range of 95 to 100 W/cm^2. It can be seen that HfO_2-5 mol% Y_2O_3 (5YSHf) had a significant conductivity increase upon the 1650 °C thermal exposure even after only a couple of hours testing. On the other hand, the HfO_2-15 mol% Y_2O_3 (15YSHf) and HfO_2-25 mol% Y_2O_3 (25YSHf) coatings showed lower initial and 20-h sintered thermal conductivity, indicating the better temperature stability of the higher dopant coatings. The x-ray diffraction results showed that the as-sprayed 5YSHf coating initially had a partially stabilized tetragonal phase structure with a small amount of the monoclinic phase (2 to 3 mol%). The as-sprayed 15YSHf and 25YSHf had a stabilized cubic structure. The monoclinic phase content in the 5YSHf coating increased to 10 to 12 mol% after the 1650 °C testing. Therefore, the conductivity increase for the 5YSHf coating is not only due to the significant sintering of the coating, but also to the increased amount of the higher conductivity monoclinic phase in the coating. Advanced multicomponent HfO_2 coatings (containing multiple rare earth dopants) have been developed that have achieved even lower thermal conductivity and better thermal stability (refs. 8 and 10).

Figure 5 shows thermal conductivity change kinetics of plasma-sprayed zirconate and/or hafnate (pyrochlore oxide) and magnetoplumbite coatings tested at 1600 to 1630 °C (with the pass-through heat flux of 100 W/cm^2). The zirconate and/or hafnate coatings showed significantly lower thermal conductivity than the magnetoplumbite oxide coatings. The development of advanced pyrochlore coatings is also in progress to further improve the coating toughness, thermal stress resistance and overall performance.

Figure 6 shows the 1650 °C sintering and cyclic behavior of the HfO_2-18 mol% $(Y,Gd,Yb)_2O_3$ coating compared with 5YSHf and 15YSHf coatings. The advanced multicomponent HfO_2-based coating had a relatively low conductivity increase during the first 20 hr of steady-state testing. It also showed essentially no cracking and delamination during subsequent testing for 100 30-min cycles at 1650 °C, indicating excellent sintering resistance and cyclic durability. In contrast, the HfO_2 baseline coatings showed significant conductivity increases during the initial 20-hr steady-state sintering test and then conductivity reductions during thermal cycling because the coating had cracked and delaminated. The 5YSHf showed severe spallation partially because of the large amount of monoclinic phase formation (>25 mol%) and phase destabilization (ref. 3).
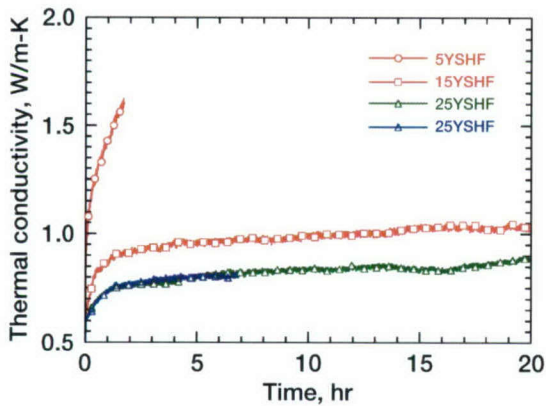
Figure 4.—Thermal conductivity of plasma-sprayed HfO_2-Y_2O_3 coatings tested at 1650 °C as function of time with pass-through heat flux of 95 to 100 W/cm^2.
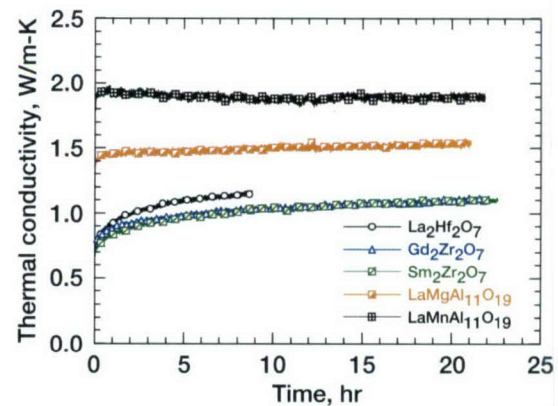

Figure 5.—Thermal conductivity of plasma-sprayed zirconate/hafnate and magnetoplumbite coatings tested at 1600 to 1620 °C with pass-through heat flux of 100 W/cm^2.
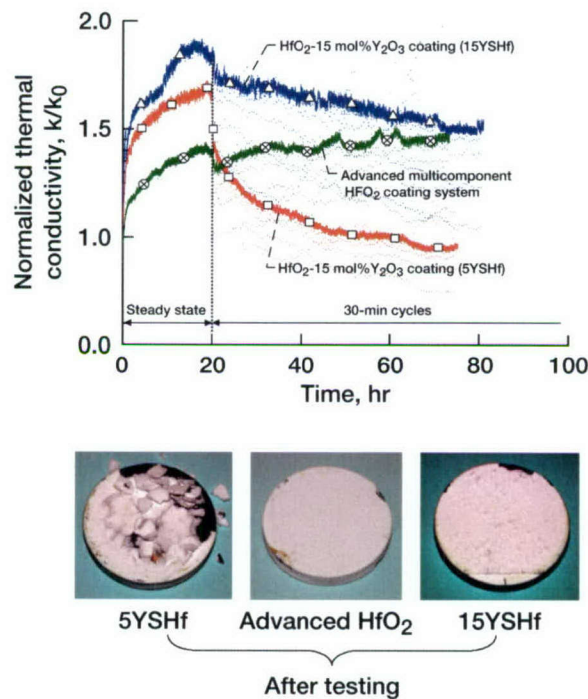

5YSHf   Advanced HfO_2 15YSHf

After testing

Figure 6.—Thermal conductivity of multicomponent HfO_2/mullite-based coating system compared with baseline 5YSHf/mullite and 15YSHf/mullite coatings, all on Hexoloy SiC substrates under 1650 °C thermal gradient cyclic testing.

Figure 7 illustrates the long-term durability exhibited by the multicomponent HfO_2-18 mol% $(Y,Gd,Yb)_2O_3$ coating system coated on mullite/mullite+20%BSAS/Si during 1650 °C thermal cycling. It can be seen that the multicomponent HfO_2-18 mol% $(Y,Gd,Yb)_2O_3$/mullite-based thermal and environmental barrier coating systems demonstrated 300-hr long-term 1650 °C sintering and cyclic durability on SiC/SiC ceramic matrix composites under the thermal gradient cyclic testing conditions. Further advanced coating development is underway to further improve the coating temperature capability and durability under simulated engine combustion environments.
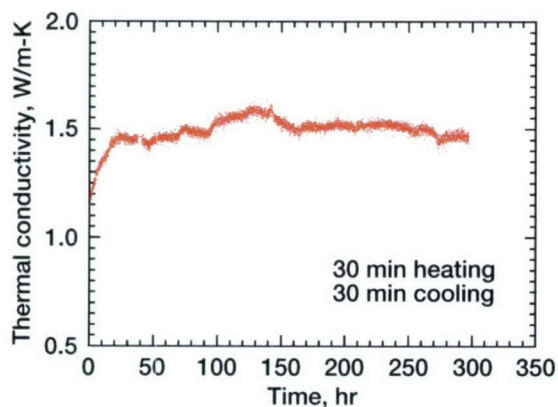
Figure 7.—Thermal conductivity of multicomponent HfO$_2$/mullite-based coating system on SiC/SiC CMC under 1650 °C thermal gradient cyclic testing for 300 hr.
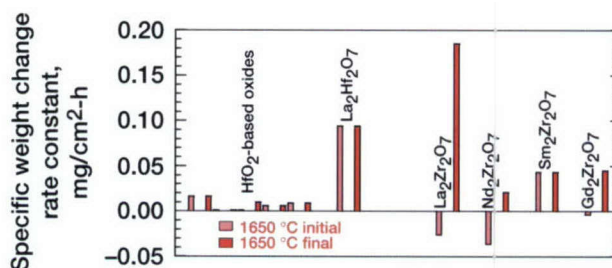

Figure 8.—Water vapor stability of selected HfO$_2$-based and pyrochlore oxides, determined by thermogravimetric analysis in 50-50% flowing water vapor-oxygen environment at 1650 °C.

Water Vapor Stability

Figure 8 shows the water vapor stability of selected HfO$_2$-based and pyrochlore oxides, determined by TGA in a 50-50 percent flowing water vapor-oxygen environment at 1650 °C. It can be seen that the HfO$_2$ oxides showed very good water vapor resistance without weight loss and only a slight weight gain after the 100-h TGA water vapor testing. X-ray diffraction also showed no phase change or other phase contaminations after the testing. The minor weight gain of the HfO$_2$ was attributed to some possible OH$^-$ incorporation into the oxide system, as was later confirmed from the increased oxygen concentration (reduced oxygen deficiencies) within the oxides by scanning electron microscopy-energy dispersive spectroscopy (SEM/EDS) analyses. The pyrochlore oxides Sm$_2$Zr$_2$O$_7$, Gd$_2$Zr$_2$O$_7$, and La$_2$Hf$_2$O$_7$ seemed to be stable and showed some weight gains after the water vapor testing. The La$_2$Zr$_2$O$_7$ and Nd$_2$Zr$_2$O$_7$ had initial weight losses in the first 10 to 20 h of testing, suggesting the water vapor attack vulnerability at this temperature. The large weight gains of these pyrochlore oxides in the late stage of the tests are found to be related to some reaction products formed when the specimens reacted with the environments. The alumina furnace tube likely reacts with water vapor to form Al(OH)$_3$ (ref. 11), which effects sample weight gain (e.g., postexposure x-ray diffraction of La$_2$Zr$_2$O$_7$ also shows LaAlO$_3$).

The water vapor TGA test for one of the magnetoplumbite oxides (LaMnAl$_{11}$O$_{19}$) showed a significant weight loss (–0.037 mg/cm^2·h) even at 1500 °C, indicating the poor water vapor stability of the oxide material. Further studies may be necessary to investigate the water vapor stability of other rare earth-doped magnetoplumbite oxides.

Conclusions

Advanced HfO$_2$, pyrochlore, and magnetoplumbite oxides are being developed for 1650 °C (3000 °F) thermal and environmental barrier coatings for low-emission SiC/SiC ceramic matrix composite (CMC) combustor and vane applications. Rare earth doping and composition optimization have demonstrated an effective approach for reducing material thermal conductivity as well as improving thermal and water vapor stability. Multicomponent, co-doped oxide systems generally showed better performance. HfO$_2$ and certain pyrochlore oxides are promising candidate materials for the 1650 °C coatings because of their low thermal conductivity and good high-temperature stability in oxidizing and water-vapor-containing combustion environments. Further studies are needed to investigate magnetoplumbite materials for the

high-temperature coating applications. The thermal gradient cyclic tests also demonstrated the 1650 °C coating feasibility and capability for the potential higher temperature SiC/SiC CMC engine component applications.

References

1. Zhu, Dongming; and Miller, Robert A.: Thermal Conductivity Change Kinetics of Ceramic Thermal Barrier Coatings Determined by the Steady-State Laser Heat Flux Technique. Research & Technology 1999, NASA/TM—2000-209639, 2000, pp. 29–31.
2. Zhu, D.M.; and Miller, R.A.: Thermal Conductivity and Elastic Modulus Evolution of Thermal Barrier Coatings Under High Heat Flux Conditions. J. Therm. Spray Technol., vol. 9, no. 2, 2000, pp. 175–180.
3. Zhu, Dongming; and Miller, Robert A.: Development of Advanced Thermal and Environmental Barrier Coatings Using a High-Heat-Flux Testing Approach. Paper presented at the 27th Annual International Conference on Advanced Ceramics and Composites, Cocoa Beach, FL, 2003.
4. Zhu, D., et al.: Thermal Conductivity of Ceramic Coating Materials Determined by a Laser Heat Flux Technique. High Temperature Ceramic Matrix Composites, W. Krenkel, R. Naslain, and H. Schneider, eds., Wiley-VCH, New York, NY, 2001, pp. 262–267.
5. Zhu, D.M.; and Miller, R.A.: Thermal-Barrier Coatings for Advanced Gas-Turbine Engines. MRS Bulletin, vol. 25, no. 7, 2000, pp. 43–47.
6. Zhu, D.M.; Lee, K.N.; and Miller, R.A.: Thermal Conductivity and Thermal Gradient Cyclic Behavior of Refractory Silicate Coatings on SiC/SiC Ceramic Matrix Composites. Ceram. Eng. Sci. Proc., vol. 22, no. 4, 2001, pp. 443–452.
7. Zhu, D.; and Miller, R.A.: Thermophysical and Thermomechanical Properties of Thermal Barrier Coating Systems. Ceram. Eng. Sci. Proc., vol. 21, no. 4, 2000, pp. 623–633.
8. Zhu, D.M.; Bansal, N.P.; and Miller, R.A.: Thermal Conductivity and Stability of HfO_2-Y_2O_3 and $La_2Zr_2O_7$ Evaluated for 1650 °C Thermal/Environmental Barrier Coating Applications. Ceram. Trns., vol. 153, 2003, pp. 331–343.
9. Opila, E.J.: Oxidation Kinetics of Chemically Vapor-Deposited Silicon Carbide in Wet Oxygen. J. Am. Ceram. Soc., vol. 77, no. 3, 1994, pp. 730–736.
10. Zhu, Dongming; and Miller, Robert A.: Thermal Conductivity of Advanced Ceramic Thermal Barrier Coatings Determined by a Steady-State Laser Heat-Flux Approach. Proceedings of the 27th International Thermal Conductivity Conference and the 15th International Thermal Expansion Symposium, Hsin Wang and Wallace Porter, eds., DEStech Publications, Inc., Lancaster, PA, 2004, pp. 291–303.
11. Opila, E.J.; and Myers, D.: Alumina Volatility in Water Vapor at Elevated Temperatures: Application to Combustion Environments. 2003 Proceedings Volume 2003–16, The Electrochemical Society, Inc., Meeting, Paris, France, 2003, pp. 535–544.

REPORT DOCUMENTATION PAGE

1. AGENCY USE ONLY (*Leave blank*)	2. REPORT DATE December 2004	3. REPORT TYPE AND DATES COVERED Technical Memorandum

4. TITLE AND SUBTITLE

Advanced Oxide Material Systems for 1650 °C Thermal/Environmental Barrier Coating Applications

6. AUTHOR(S)

Dongming Zhu, Dennis S. Fox, Narottam P. Bansal, and Robert A. Miller

5. FUNDING NUMBERS

WBS–22–714–20–09
1L161102AF20

7. PERFORMING ORGANIZATION NAME(S) AND ADDRESS(ES)

National Aeronautics and Space Administration
John H. Glenn Research Center at Lewis Field
Cleveland, Ohio 44135–3191

8. PERFORMING ORGANIZATION REPORT NUMBER

E–14726

9. SPONSORING/MONITORING AGENCY NAME(S) AND ADDRESS(ES)

National Aeronautics and Space Administration
Washington, DC 20546–0001
and
U.S. Army Research Laboratory
Adelphi, Maryland 20783–1145

10. SPONSORING/MONITORING AGENCY REPORT NUMBER

NASA TM—2004-213219
ARL–TR–3298

11. SUPPLEMENTARY NOTES

12a. DISTRIBUTION/AVAILABILITY STATEMENT

Unclassified - Unlimited
Subject Categories: 23, 24, and 27   Distribution: Nonstandard

Available electronically at http://gltrs.grc.nasa.gov

This publication is available from the NASA Center for AeroSpace Information, 301–621–0390.

12b. DISTRIBUTION CODE

13. ABSTRACT (*Maximum 200 words*)

Advanced thermal and environmental barrier coatings (TEBCs) are being developed for low-emission SiC/SiC ceramic matrix composite (CMC) combustor and vane applications to extend the CMC liner and vane temperature capability to 1650 °C (3000 °F) in oxidizing and water-vapor-containing combustion environments. The advanced 1650 °C TEBC system is required to have a better high-temperature stability, lower thermal conductivity, and more resistance to sintering and thermal stress than current coating systems under engine high-heat-flux and severe thermal cycling conditions. In this report, the thermal conductivity and water vapor stability of selected candidate hafnia-, pyrochlore- and magnetoplumbite-based TEBC materials are evaluated. The effects of dopants on the materials' properties are also discussed. The test results have been used to downselect the TEBC materials and help demonstrate the feasibility of advanced 1650 °C coatings with long-term thermal cycling durability.

14. SUBJECT TERMS

Thermal barrier coating; Environmental barrier coating; Thermal conductivity; Ceramic matrix composites; Water vapor stability

15. NUMBER OF PAGES
14

16. PRICE CODE

17. SECURITY CLASSIFICATION OF REPORT Unclassified	18. SECURITY CLASSIFICATION OF THIS PAGE Unclassified	19. SECURITY CLASSIFICATION OF ABSTRACT Unclassified	20. LIMITATION OF ABSTRACT